

Precession and Split of Tilted, Geometrically Thin Accretion Disk: an Analytical Study

Ye Shen,^{1*} Bin Chen^{1,2,3*†}

¹*School of Physics, Peking University, No.5 Yiheyuan Rd, Beijing 100871, P. R. China*

²*Center for High Energy Physics, Peking University, No.5 Yiheyuan Rd, Beijing 100871, P. R. China*

³*Collaborative Innovation Center of Quantum Matter, No.5 Yiheyuan Rd, Beijing 100871, P. R. China*

April 11, 2024

Abstract

It has been observed that many relativistic jets display a kind of cork-screw-like precession. Numerical simulations has suggested that such kind of precession may originate from the precession of the disk. In this work, we introduce an analytical model to describe the precession and split of a tilted, geometrically thin disk. We consider the Lense-Thirring effect from the central (primary) black hole (BH) and the gravitational effect from the companion (secondary) BH far away from the center, both of which could induce the precession of the accretion disk around the spin axis of central black hole. We propose the splitting conditions that when the rate of viscous diffusion cannot catch up with the dynamical frequency at a certain layer of fluid, the disk would split into two parts which precess independently. We presume that the precessions of the inner and outer disks are in accord with the rotation and precession of jet, respectively. By matching the frequencies of the disks to the observed frequencies of jet in the cork-screw-like precession and considering the splitting condition, we are allowed to read four parameters, the innermost radius (r_{in}), the outermost radius (r_{out}) of the disk, the initial splitting radius ($r_{\text{sp},0}$), and the inflow speed magnitude(β), of the disk. We apply this model to OJ 287. Moreover, considering the inward shrinking of the disks, we find the time variation of the precession angle of jet. This time variation presents a unique feature of our model, which could be distinguishable in the future observation.

Keywords– Tilted Disk – Disk Precession – AGN – OJ 287

*E-mail: shenye199594@stu.pku.edu.cn

†E-mail: bchen01@pku.edu.cn

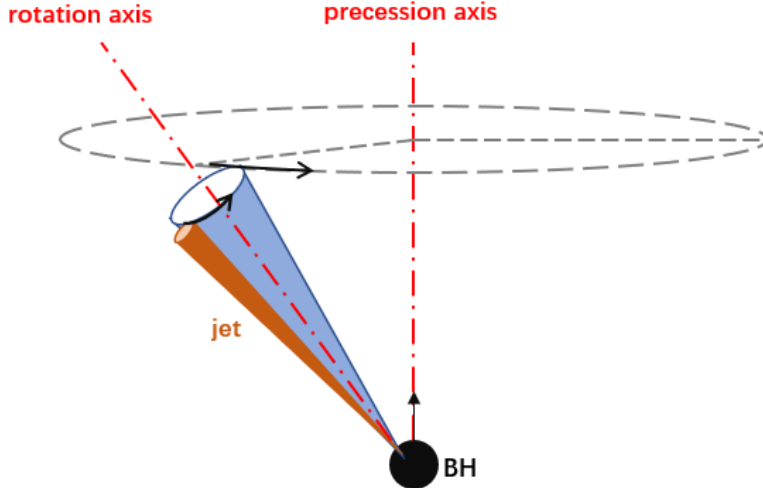


Figure 1: Scheme of cork-screw-like precession.

1 Introduction

Relativistic jet, one of the components in accretion system, is one of the most important topics on active galactic nuclei (AGN). Time variation of radiations has been recognized as one of the main characteristics of AGN, especially for blazar and BL Lac whose relativistic jets are regarded to shoot almost towards observers [1]. A set of sources were observed to be time varying in the early 21st century, such as 3C 345 and 3C 120 [2–4], and their quasi-periodic variations were ascribed to the precession of jet along axis of BH spin. In some studies, it has been suggested that the precession of jet comes from that of accretion disk, even though it is still unclear whether and how the motion of the disk is transferred to the jet [5, 6].

Recent observations, which focus on the positions of the heads of jets, make it more trustworthy that the time variation of radiations comes from jet precession. Moreover, better refined observations, especially those on OJ 287 [7, 8], showed a quasi-periodic oscillation of jet with two periods. These observations indicate that the jet may not simply precess as what assumed before. Instead, the jet could move in a more complicated way. In the so-called cork-screw-like precession [9], a jet rotates along an axis which precesses along the spin axis of BH (see Fig. 1). The period of jet rotation is generally much smaller than that of precession, which makes the jet head move in a helical way. Similar phenomena were also observed in M81 [9–11], M87 [12] and 3C 84 [13]. Fitting the observed data to the cork-screw-like precession helps us to determine the periods of both jet rotation and precession.

The origin of the cork-screw-like precession of jet remains a mystery. As widely known, both Blandford-Znajek mechanism (BZ) and Blandford-Payne mechanism (BP) may successfully describe how the jet forms by twisting large-scale magnetic field lines penetrating central BH (in BZ) or accretion disk

(in BP) [14–16]. The formation of jet could be a combined result of BZ and BP mechanisms, while many factors may influence their dominations. If the BH spin is not so fast and the magnetic field penetrating the disk is very strong, the BP process dominates the formation of the jet. Consequently, in this case, that the motion of jet originates from the precession of disk is more acceptable, as widely assumed previously [5–8].

Theoretically, a tilted disk, whose angular momentum directs not along the spin of the central BH, would precess as the result of Lense-Thirring (LT) effect [6, 17] or the dragging of secondary BH [18]. The precession of disk induced by the spin of the central BH via the LT effect had been verified numerically from the magnetohydrodynamics (MHD) simulations [19, 20]. In recent years, the general relativistic MHD (GRMHD) simulations were made to help us better understand the disk precession intuitively, as well as the motion of jet [21–27]. Although those simulations are costly and restrictive since certain physical parameters and initial conditions have to be chosen appropriately to get desired results, they do provide us with enlightening pictures.

Important phenomena uncovered through the GRMHD simulations are concluded as follows. First, a tilted disk would precess along BH spin axis, as widely described analytically. Second, the disk would split into two or even more parts if it is geometrically thin (the empirical critical value shows $H/R \lesssim 0.03$) and each parts (we call the inner and outer disk if the disk splits up into two parts) would precess independently [21, 27]. Third, the outer part of the jet ($\gtrsim 100GM/c^2$) moves along a trajectory that is closely helical, as we can see from the oscillations of its nutation and precession angle [25]. It means that the numerical results support the cork-screw-like precession. Fourth, the jet is bent [22, 23]. More importantly, the inner part of jet would generally moves synchronously to the precession of inner disk while the outer part of jet would generally moves synchronously to the precession of outer disk, which finally makes the bent structure [25, 26]. This phenomenon establishes a robust relation between the precessions of different parts of disk and the motions of jet. Fifth, the inner disk, on which the plasma is accreted to the central BH, would gradually shrink and finally disappea. What is more, the inner boundary of the outer disk would contract together with the shrinking of the inner disk. After the inner disk has been totally absorbed into the central BH, the outer disk returns to the unsplit case and then a new splitting could happen after a while [27].

As the GRMHD simulations suggested that the observed helical motion of jet could originate from the precession of disk, we might be able to precisely describe the motion of jet by analyzing the precessions of different parts of disk. In this work, we provide an analytical model to describe the precession and split of an accretion disk. We start from relativistic standard disk, an analytical model of accretion disk with geometrically thin structure, and give it a tiny tilt with respect to the equatorial plane. We basically assume that the disk would split into two parts which precess independently under certain splitting conditions. The inner part which precesses faster corresponds to the rotation of the jet while the outer part which precesses slower corresponds to the precession of the jet. The inward movement of the inner disk (and of the inner boundary of the outer disk) makes the precession periods vary with time.

We simply fit the time-averaged periods of disk to the two periods of jet in cork-screw-like precession. Together with the splitting conditions, we finally get four equations to determine four parameters of the disk: the innermost (r_{in}) and the outermost radius (r_{out}), the initial split radius ($r_{\text{sp},0}$) and the inflow speed magnitude(β). The three radii above tell the regions of accretion disk, while the inflow speed magnitude tells how fast the disk is accreted to the central BH, as well as how strong the chaotic magnetic field and turbulent flow acting on angular momentum transfer should be [28–30]. As we know, it is always much harder to measure the parameters of disk than those of jet since jet is much larger and brighter. It would be surprising if we can determine some parameters of the disk by observing the corresponding jet directly.

The remaining parts of the paper is organized as follows. In Sect. 2, we describe our model in detail, including basic assumptions and process in Sect. 2.1, the disk precession in Sect. 2.2, the structure of disk we choose in Sect. 2.3, the splitting conditions in Sect. 2.4, and determining the parameters of disk in Sect. 2.5. We apply the model to the study of OJ 287 in Sect. 3. Finally, in Sect. 4, we summarize our work and make some discussions. Some technical details are put into Appendix. In the following we set $G = M = c = 1$, where M is the mass of central BH.

2 Model description

2.1 Basic setup and process

In this section, we introduce an analytical model which describes the precession and split of a tilted disk. We start with the Novikov-Thorne model [31, 32], which analytically describes an axially symmetric and geometrically thin accretion disk around a Kerr BH (see Sect. 2.3 for details). We assume that the tilted angle is tiny ($\alpha_{\text{tilt}} \ll 1$) so that the disk keeps its structure. This approximation is suitable since the predicted tilted angles of jet from observations are not larger than $\sim 10^\circ$ for OJ 287 [7, 8], M81 [9] and M87 [12]. We consider two gravitational effects which induce the precession of disk: the Lense-Thirring effects coming from the primary BH and the torque given by the secondary BH.

The accretion disk can be taken as viscous fluid. Different layers of fluid are stucked by the viscosity when precessing, while each layer of fluid rotates around the primary BH independently in Keplerian motion. Namely, we generally have: $t_{\text{prec}} \gtrsim t_{\text{vis}} \gg t_{\text{K}}$, where t_{prec} denotes the period of precession, t_{vis} is the viscous timescale and t_{K} the Keplerian period. However, the disk would split into two parts (as we hope) on a special radius $r_{\text{sp},0}$, named initial split radius, where the dynamical timescale of precession is comparable to the viscous timescale (see Sect. 2.4 for the splitting condition). We simply assume that no other deformation of disk exists in this model. After the splitting, two split disks would precess independently. The precession frequencies of the inner disk and the outer disk are assumed to correspond to the rotation frequency $\Omega_{\text{r,obs}}$ and precession frequency $\Omega_{\text{p,obs}}$ of jet in cork-screw-like precession, respectively. The rationality of this assumption will be discussed in Sect. 4. While the outer

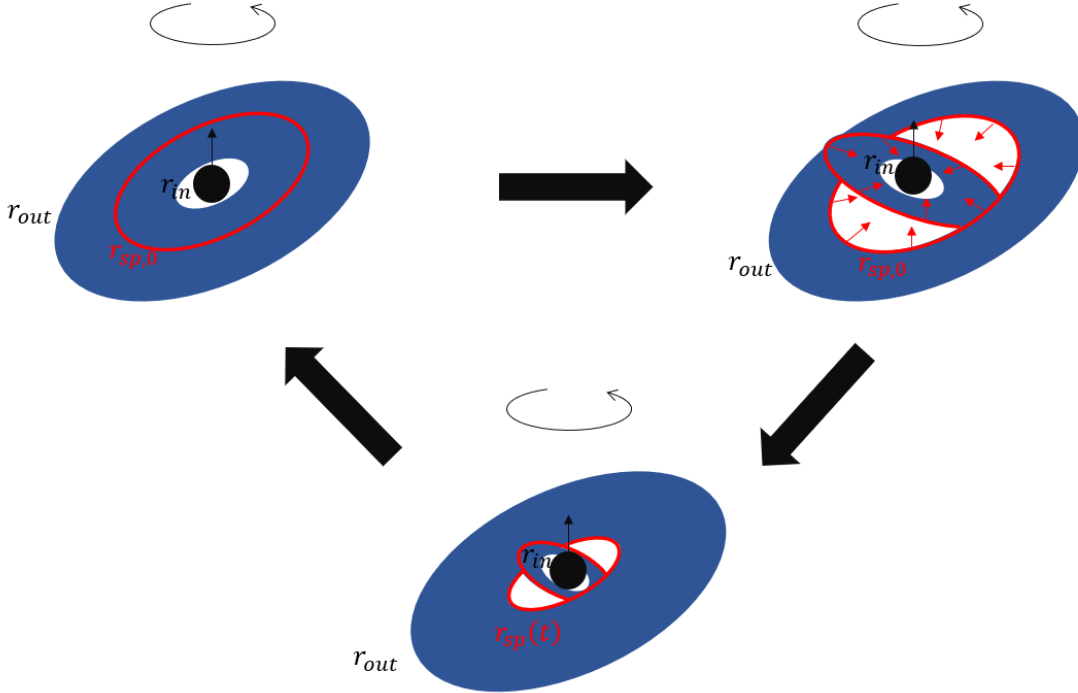


Figure 2: Process of disk precession and split.

radius of the inner disk would decrease, until the inner disk disappear.

The whole process is depicted in Fig. 2. The geometrically thin disk ranges from r_{in} to r_{out} , and its axis of precession is parallel to primary BH spin. The disk would split at $r_{\text{sp},0}$, and then the part within $r_{\text{sp},0}$, which we call the inner disk, and the part out of $r_{\text{sp},0}$, which we call the outer disk, would precess independently. Because of accretion, the inner disk would shrink, together with the inward movement of inner boundary of the outer disk. We simply assume that the inner radius of the outer disk is always the same as the outer radius of the inner disk, noted as $r_{\text{sp}}(t)$. This assumption is strongly supported by numerical results [27]. Additionally, There would be no interaction between the inner disk and the outer disk. When the inner disk is wholly absorbed into the central BH, the outer disk becomes a new, unsplit disk. Namely, the accretion disk returns back to the initial structure. Then the disk again splits into two parts, following the same process stated above.

2.2 Precession frequency

We consider two kinds of effect which could cause the precession of tilted accretion disk. One is the Lense-Thirring effects due to the rotation of primary BH, the other is the gravitational perturbation of a secondary BH locating on the equatorial plane with a separation R much larger than the scale of accretion disk. Both of the effects lead to a precession parallel to spin axis of primary BH.

We firstly consider a massive fluid ring that is assumed to be steady, rotating around the central BH on a certain radius r with a Keplerian velocity. Its angular frequency of precession, caused by the

Lense-Thirring effects, is [17]:

$$\omega_{\text{p,LT}} = \Omega_{\text{K}} \left[1 - \left(1 - 4ar^{-3/2} + 3a^2r^{-2} \right)^{1/2} \right] \quad (2.1)$$

where $\Omega_{\text{K}} = (r^{3/2} + a)^{-1}$ is the Keplerian frequency. We can easily see that $\omega_{\text{p,LT}} = 0$ when $a = 0$, which tells that no precession happens if primary BH has no spin. Also, the precession frequency reduces to the weak field case $\omega_{\text{p,LT}} \sim 2ar^{-3}$ [33] when $r \gg 1$. A detailed analysis is shown in Appen. A.1.

The angular frequency of precession of this massive ring caused by the secondary BH on the equatorial plane is [18]:

$$\omega_{\text{p,q}} = -\frac{3q}{4R^3\Omega_{\text{K}}} \cos \alpha_{\text{tilt}} \quad (2.2)$$

by assuming that the Keplerian frequency of secondary BH is much smaller than that of massive ring while is much larger than its precession frequency. Here q is the mass ratio of secondary BH to the primary one and R is the separation between the primary and secondary BH. If the separation between primary and secondary BH is much larger than the disk scale, the Keplerian frequency of secondary BH can be much smaller than that of disk. On the other hand, the Keplerian frequency of secondary BH could be not larger than the precession frequency of massive ring if the radius of the ring is small. However, the effect of secondary BH on a ring with small radius is negligible so that we do not need to worry about this case. More detailed discussions on the precession due to a secondary BH can be found in Appen. A.2.

Taking both effects into account, we find that the total precession frequency of a massive ring with radius r is just:

$$\omega_{\text{p}} = \omega_{\text{p,LT}} + \omega_{\text{p,q}}. \quad (2.3)$$

Now let us consider the the precession frequency of disk ranging from r_1 to r_2 . We require $t_{\text{prec}} \gtrsim t_{\text{vis}} \gg t_{\text{K}}$, such that different layers of massive fluid ring rotate around the central BH independently while precess about the spin axis of central BH as an entire body due to viscosity [34]. Additionally, we assume that there is no other effect to change the shape of the disk [34, 35]. Consider the gravitational torque, which causes the precession, acting on this entire body. It should be the summation of torques acting on fluid elements:

$$\tau_{\text{tot}} = \int_{\mathcal{V}} \omega_{\text{p}} J_{\tilde{\phi}} \sqrt{\gamma} dr d\theta d\phi. \quad (2.4)$$

Here $J_{\tilde{\phi}}$ is the angular momentum of fluid element while $\tilde{\phi}$ denotes the rotation direction. \mathcal{V} denotes the spatial region of the accretion disk. And γ is the determinant of the induced metric. The total torque could also be the angular momentum of the entire body multiplied by the uniform angular frequency of precession, namely:

$$\tau_{\text{tot}} = \Omega_{\text{p}} J_{\text{tot}} = \Omega_{\text{p}} \int_{\mathcal{V}} J_{\tilde{\phi}} \sqrt{\gamma} dr d\theta d\phi \quad (2.5)$$

Equating Eq. (2.4) and (2.5), we get (see also [6, 34]):

$$\Omega_{\text{p}} = \frac{\int_{\mathcal{V}} \omega_{\text{p}} J_{\tilde{\phi}} \sqrt{\gamma} dr d\theta d\phi}{\int_{\mathcal{V}} J_{\tilde{\phi}} \sqrt{\gamma} dr d\theta d\phi}. \quad (2.6)$$

Formally, the precession frequency of the disk is just an average of precession frequencies of each fluid element weighted by angular momentum.

If the tilted angle is tiny, we could approximately have:

$$J_{\tilde{\phi}} \approx J_{\phi} = T_{\phi}^t \approx \rho u^t u_{\phi}. \quad (2.7)$$

The second "≈" in Eq. (2.7) is plausible in the case that the internal and electromagnetic energy is much smaller than inertial mass, which holds in general in accretion disk. Since the disk we consider is axially symmetric and geometrically thin, we can do the integration along θ and ϕ in Eq. (2.6) so that

$$\begin{aligned} \Omega_{\text{p}}[r_1, r_2] &= \frac{\int_{r_1}^{r_2} \omega_{\text{p}} \rho H r^{-1} u^t u_{\phi} \sqrt{\gamma_{\theta=\frac{\pi}{2}}} dr}{\int_{r_1}^{r_2} \rho H r^{-1} u^t u_{\phi} \sqrt{\gamma_{\theta=\frac{\pi}{2}}} dr} \\ &= \frac{\int_{r_1}^{r_2} \omega_{\text{p}} \Sigma_{\text{d}} r^{-1} u^t u_{\phi} \sqrt{\gamma_{\theta=\frac{\pi}{2}}} dr}{\int_{r_1}^{r_2} \Sigma_{\text{d}} r^{-1} u^t u_{\phi} \sqrt{\gamma_{\theta=\frac{\pi}{2}}} dr}, \end{aligned} \quad (2.8)$$

where $\Sigma_{\text{d}} = \rho H$ is the surface density of the disk. With Eq. (2.8), the angular frequency of disk is just a function of inner and outer radii of the disk. In a Kerr spacetime, we have

$$\sqrt{\gamma_{\theta=\frac{\pi}{2}}} = r^2 \sqrt{\frac{r^2 + 2a^2 r + a^2}{r^2 - 2r + a^2}}, \quad (2.9)$$

and also

$$\begin{aligned} u^t &= \frac{r^{\frac{3}{2}} + a}{\sqrt{r^3 - 3r^2 + 2ar^{\frac{3}{2}}}}, \\ u_{\phi} &= \frac{r^2 - 2ar^{\frac{1}{2}} + a^2}{\sqrt{r^3 - 3r^2 + 2ar^{\frac{3}{2}}}} \end{aligned} \quad (2.10)$$

for Keplerian orbits.

We may define three useful functions as following:

$$\Omega_{\text{in}}(t) = \Omega_{\text{p}}[r_{\text{in}}, r_{\text{sp}}(t)] \quad (2.11)$$

the precession frequency of inner disk,

$$\Omega_{\text{out}}(t) = \Omega_{\text{p}}[r_{\text{sp}}(t), r_{\text{out}}] \quad (2.12)$$

the precession frequency of outer disk, and

$$\Delta\Omega_{\text{p}}(r) = \Omega[r_{\text{in}}, r] - \Omega[r, r_{\text{out}}] \quad (2.13)$$

the difference of angular frequencies between inner and outer disks if the disk splits at a radius r . The time dependence of Ω_{in} and Ω_{out} comes from the inward movement of split radius, as mentioned in Sect. 2.1. See Sect. 2.4 for the expression of $r_{\text{sp}}(t)$

2.3 Disk structure: Novikov-Thorne disk

We choose the Novikov-Thorne (NT) disk [31, 32], the so-call relativistic standard disk, to describe the disk structure in our model. Its non-relativistic approximation [28] is also widely used to describe a geometrically thin but optically thick disk. In the NT model, the disk can be divided into three distinct regions [28]: the inner region where the radiative pressure (P_{rad}) is much larger than the gas pressure (P_{gas}) and the Thomson scattering is dominant for opacity, the medium region where P_{gas} is much larger than P_{rad} and the Thomson scattering is dominant, and the outer region where P_{gas} is much larger than P_{rad} while free-free absorption is dominant. However, further researches showed that the disk in the inner region should be secularly unstable [36] or thermally unstable [37]. Resultantly, the disk cannot keep a geometrically thin structure in the inner region. What is more, the outer region is so far away from the central BH ($r \gtrsim 10^3 r_g$) that the magnetic field in the outer regions has nothing to do with the magnetic field in the jet. For the reasons mentioned above, we focus on the medium region only. Details about the inner region of the disk will be discussed in Sect. 4.

Apart from the angular frequency of each layer of fluid, we need the surface density, radial velocity and viscous timescale as well, which are expressed as

$$\Sigma_{\text{d}}(r) = \Sigma_{\text{d},0} r^{-\frac{3}{5}} \mathcal{B}^{-\frac{3}{5}} \mathcal{C}^{\frac{1}{2}} \mathcal{D}^{-\frac{4}{5}} \mathcal{Q}^{\frac{3}{5}}, \quad (2.14)$$

$$v^r(r) = -\frac{\beta}{4\pi} r^{-\frac{2}{5}} \mathcal{B}^{\frac{3}{5}} \mathcal{C}^{-\frac{2}{3}} \mathcal{D}^{-\frac{1}{5}} \mathcal{Q}^{-\frac{3}{5}}, \quad (2.15)$$

and [29]

$$t_{\text{vis}} = \frac{\pi r^2 \Sigma_{\text{d}}}{\dot{M}} = -\frac{r}{2v^r \mathcal{D}^{\frac{1}{2}}}. \quad (2.16)$$

Here $\Sigma_{\text{d},0}$ and β are two undetermined coefficients. With the viscous timescale, we can define viscous frequency as

$$\Omega_{\text{vis}}(r) = \frac{2\pi}{t_{\text{vis}}} = \beta r^{-\frac{7}{5}} \mathcal{B}^{\frac{3}{5}} \mathcal{C}^{-\frac{2}{3}} \mathcal{D}^{\frac{3}{10}} \mathcal{Q}^{-\frac{3}{5}}. \quad (2.17)$$

Note that our model is independent of $\Sigma_{\text{d},0}$, as we can see from Eq. (2.8). In other words, our model cannot restrict the value of $\Sigma_{\text{d},0}$.

The r -dependent functions \mathcal{B} , \mathcal{C} , \mathcal{D} and \mathcal{Q} are relativistic factors for circular orbit in Kerr spacetime. They take the following specific forms:

$$\begin{aligned} \mathcal{B} &= 1 + ar^{-3/2}, \\ \mathcal{C} &= 1 - 3r^{-1} + 2ar^{-3/2}, \\ \mathcal{D} &= 1 - 2r^{-1} + a^2r^{-2}, \\ \mathcal{Q} &= \dots \simeq 1 - \left(l_{\text{isco}} + 3r_{\text{isco}}^{-1/2}\right)r^{-1/2} + 6r^{-1} + \dots, \end{aligned} \quad (2.18)$$

where r_{isco} and l_{isco} are the radius and specific angular momentum of innermost stable circular orbit (ISCO). Obviously all of the functions in Eq. (2.18) converge to 1 asymptotically. Because the exact form of \mathcal{Q} is too complicated, we expand it by orders of $r^{-1/2}$ and keep only the first two terms.

2.4 The splitting condition and inward movement

As we mentioned before, the viscosity is capable of gluing all layers of fluid and make them precess as an entire body. The disk does not split, as long as different parts of disk could communicate with each other through viscous diffusion on a timescale (t_{vis} in Eq. (2.16)) less than the dynamical period ($2\pi/\Delta\Omega_{\text{p}}$ with $\Delta\Omega_{\text{p}}$ in Eq. (2.13)) [34]. On the contrary, when the rate of viscous diffusion (Ω_{vis} in Eq. (2.17)) is not capable of catching up with the dynamical frequency ($\Delta\Omega_{\text{p}}$ in Eq. (2.13)) on a certain layer $r = r_{\text{sp},0}$, the disk undergoes a splitting at the layer. Concretely, over the disk which splits at $r_{\text{sp},0}$ and precesses as two independent bodies, there should be:

$$\begin{aligned}\Delta\Omega_{\text{p}}(r) &\simeq \Omega_{\text{vis}}(r) , & r = r_{\text{sp},0} \\ \Delta\Omega_{\text{p}}(r) &< \Omega_{\text{vis}}(r) , & r \neq r_{\text{sp},0}\end{aligned}\tag{2.19}$$

If both of $\Delta\Omega_{\text{p}}(r)$ and $\Omega_{\text{vis}}(r)$ are smooth, we have:

$$\begin{aligned}\frac{d}{dr}[\Delta\Omega_{\text{p}}(r) - \Omega_{\text{vis}}(r)]\Big|_{r \simeq r_{\text{sp},0}} &\simeq 0, \\ \frac{d^2}{dr^2}[\Delta\Omega_{\text{p}}(r) - \Omega_{\text{vis}}(r)]\Big|_{r \simeq r_{\text{sp},0}} &< 0.\end{aligned}\tag{2.20}$$

The equations in Eq. (2.19) and (2.20) help us to get the undetermined parameters, while the inequations restricts the trends of $\Delta\Omega_{\text{p}}(r) - \Omega_{\text{vis}}(r)$ along r . Here we expect that the disk would split on one certain radius instead of a small region around the radius which was suggested by numerical simulations [27]. It is an ideal simplification that the disk splits like a crisp biscuit rather than a soft dough.

The speed of inward movement of r_{sp} is presumed to obey Eq. (2.15). Namely, we formally have:

$$\frac{dr}{dt} = v^r(r).\tag{2.21}$$

The shrinking of the inner disk is determined by

$$t - t_0 = \int_{r_{\text{sp},0}}^{r_{\text{sp}}} \frac{dr}{v^r(r)}.\tag{2.22}$$

In one period, the inner disk forms, shrinks, and disappears at r_{in} . The period is just

$$T_{\text{sp}} = \int_{r_{\text{sp},0}}^{r_{\text{in}}} \frac{dr}{v^r(r)}\tag{2.23}$$

starting at the moment when the disk splits on $r_{\text{sp},0}$ while ending when the inner disk disappears and the disk recovers to the initial structure consequently. For simplicity, we ignore all relativistic factors in Eq. (2.15) and get

$$r_{\text{sp}}(t) = \frac{7\beta}{8\pi} \left[\frac{8\pi}{7\beta} r_{\text{sp},0}^{\frac{7}{2}} - (t - nT_{\text{sp}}) \right]^{\frac{2}{7}}, \quad n \in \mathbf{N}\tag{2.24}$$

with:

$$T_{\text{sp}} = \frac{8\pi}{7\beta} \left(r_{\text{sp},0}^{\frac{7}{2}} - r_{\text{in}}^{\frac{7}{2}} \right).\tag{2.25}$$

Substituting Eq. (2.24) and (2.25) into Eq. (2.11) and (2.12), we get the time dependence of precession frequencies of both the inner and outer disks.

2.5 Determining the parameters of disk

From the simplified model discussed above, we are ready to determine the parameters of the disk. There are totally four undetermined parameters: r_{in} , r_{out} , $r_{\text{sp},0}$ and β , among which the last one tells the strength of viscosity over the accretion disk and the former three ones tell the location and the region of disk. We need four equations to completely fix them. Recall the basic setup in Sect. 2.1 that the frequencies of the inner and outer disks ($\Omega_{\text{in}}, \Omega_{\text{out}}$) are basically assumed to correspond to the rotation and precession frequencies of jet ($\Omega_{\text{r,obs}}, \Omega_{\text{p,obs}}$). However, different from the cork-screw-like precession whose frequencies are constant, both Ω_{in} and Ω_{out} are time varying in our model. The rotation and precession of jet are assumed to be synchronous to the precessions of the inner and outer disk respectively (with a constant time lag). Consequently, the averages of Ω_{in} and Ω_{out} over time should equal to $\Omega_{\text{r,obs}}$ and $\Omega_{\text{p,obs}}$ respectively. Together with the two equations in Eq. (2.19) and (2.20), we are able to solve all undetermined parameters. In short, we need to solve the following four equations to determine $(r_{\text{in}}, r_{\text{sp},0}, r_{\text{out}}; \beta)$:

$$\begin{aligned} \frac{1}{T_{\text{sp}}} \int_0^{T_{\text{sp}}} \Omega_{\text{in}}(t) dt &\simeq \Omega_{\text{r,obs}}, \\ \frac{1}{T_{\text{sp}}} \int_0^{T_{\text{sp}}} \Omega_{\text{out}}(t) dt &\simeq \Omega_{\text{p,obs}} \end{aligned} \tag{2.26}$$

$$\begin{aligned} [\Delta\Omega_{\text{p}}(r) - \Omega_{\text{vis}}(r)] \Big|_{r \simeq r_{\text{sp},0}} &\simeq 0 \\ \frac{d}{dr} [\Delta\Omega_{\text{p}}(r) - \Omega_{\text{vis}}(r)] \Big|_{r \simeq r_{\text{sp},0}} &\simeq 0 \end{aligned}$$

Obviously there is a set of reasonable solutions obeying $r_{\text{in}} < r_{\text{sp},0} < r_{\text{out}}$. We also need to check the value of β as the relation $v^r \ll r\Omega_{\text{K}}$ has to be satisfied.

3 Results: parameters of OJ 287

We apply our model to OJ 287, a BL Lac object five billion light years away from Earth with redshift $z \simeq 0.306$ [7]. It is widely accepted that there is a supermassive BH (the primary BH) on the center with mass $M \simeq 4 \times 10^8 M_{\odot}$ [38] and a companion (secondary BH) about $10^3 r_g$ away from the central one with mass ratio $q \simeq 0.01$ [39]. We ignore the probable eccentricity and inclination of secondary BH orbit. The spin of primary BH is about 0.313 [40], such that $r_{\text{isco}} \simeq 4.39 r_g$.

The observed precession and rotation periods of jet are around 27yr and 1.6yr respectively [7, 8]. Considering the redshift, the real periods are 20yr and 1.2yr or so. Applying the mass of primary BH, we get $\Omega_{\text{r,obs}} \simeq 3.2 \times 10^{-4} t_g^{-1}$ and $\Omega_{\text{p,obs}} \simeq 1.9 \times 10^{-5} t_g^{-1}$. Taking these values into Eq. (2.26), we obtain

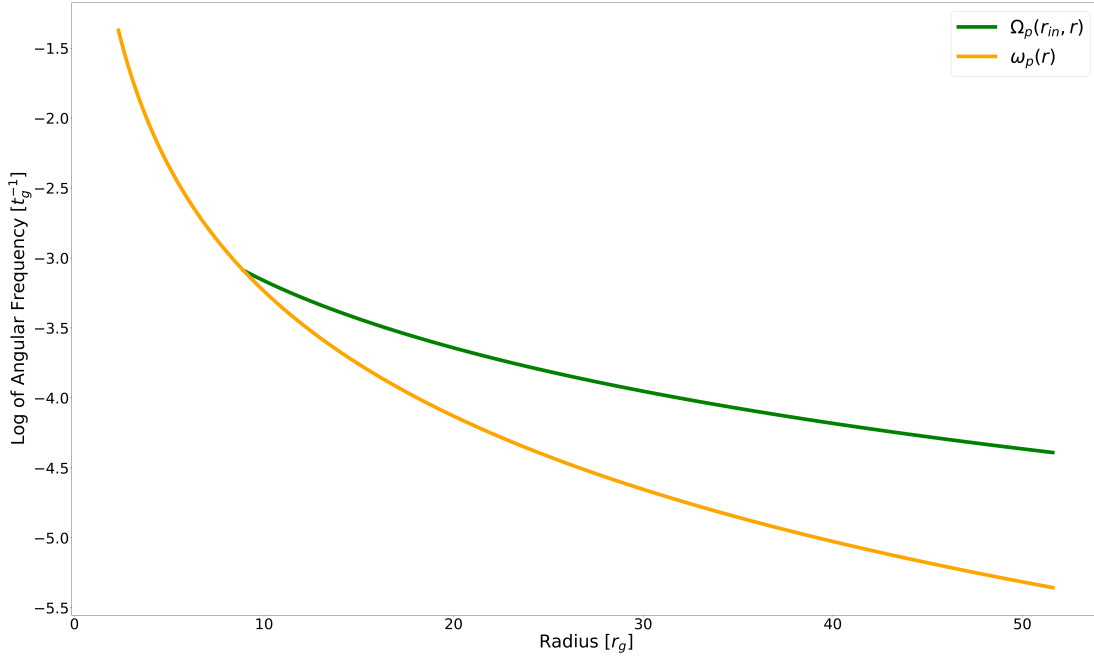


Figure 3: $\omega_p(r)$ and $\Omega_p[r_{\text{in}}, r]$ for OJ287.

$(r_{\text{in}}, r_{\text{sp},0}, r_{\text{out}}) \simeq (8.90, 26.5, 51.6)r_g$ and $\beta \simeq 6.33 \times 10^{-3}c$. The resulting period of inner disk inward movement is $T_{\text{sp}} \simeq 1.09 \times 10^5 t_g \simeq 6.80 \text{yr}$. It is 8.88yr or so after considering the redshift of OJ 287.

We plot $\omega_p(r)$ and $\Omega_p[r_{\text{in}}, r]$ in Fig. 3, using the parameters of OJ 287 we got. We can see that $\Omega_p[r_{\text{in}}, r]$ converge to the ring precession frequency when $r \rightarrow r_{\text{in}}$, as we can also see from Eq. (2.8) directly. The frequency $\omega(r_{\text{in}}) = \lim_{r \rightarrow r_{\text{in}}} \Omega_p[r_{\text{in}}, r]$ is the fastest precession frequency of the inner disk. Also, the decrease of $\Omega_p[r_{\text{in}}, r]$ along r is much slower than that of $\omega_p(r)$. Recall that the disk precession frequency is formally a weighted average of ring precession frequency such that the inner layers which have larger $\omega_p(r)$ contribute more. Physically, the inner layers of the disk could drag the outer layers to precess faster if the disk precesses as an undeformed entire body. We also compare the ring frequencies induced by the Lense-Thirring effect from primary BH and the gravitational effect from secondary BH in Fig. 4, on which the outer radius r_{out} is depicted by a dashed gray line. It is apparent that the Lense-Thirring effect is much more important over the whole accretion disk of OJ 287. So ignoring the secondary BH when considering the disk precession of OJ 287 is acceptable.

The comparison of $\Delta\Omega_p(r)$ and $\Omega_{\text{vis}}(r)$ for OJ 287 is depicted in Fig. 5, on which the gray line denotes $r_{\text{sp},0}$. When the equations and inequations in Eq. (2.19) and (2.20) are all satisfied, the disk would split at $r_{\text{sp},0}$ and precesses as two independent bodies. We can investigate the splitting of the disk further. For example, one may ask whether the inner or outer disk would split up into several parts or not? In order to answer this question, we need to compare Ω_{vis} with the dynamical frequencies defined as following

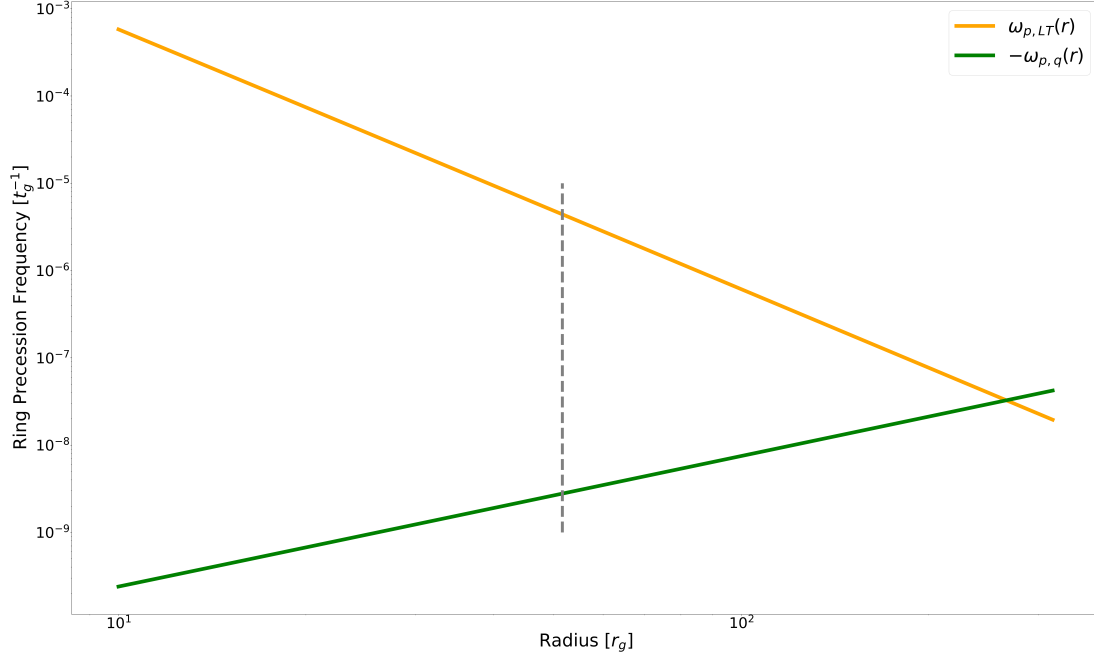


Figure 4: Ring precession frequencies induced by the Lense-Thirring effect (the orange one) and secondary BH for OJ 287 (the green one). The gray dashed line denotes r_{out} .

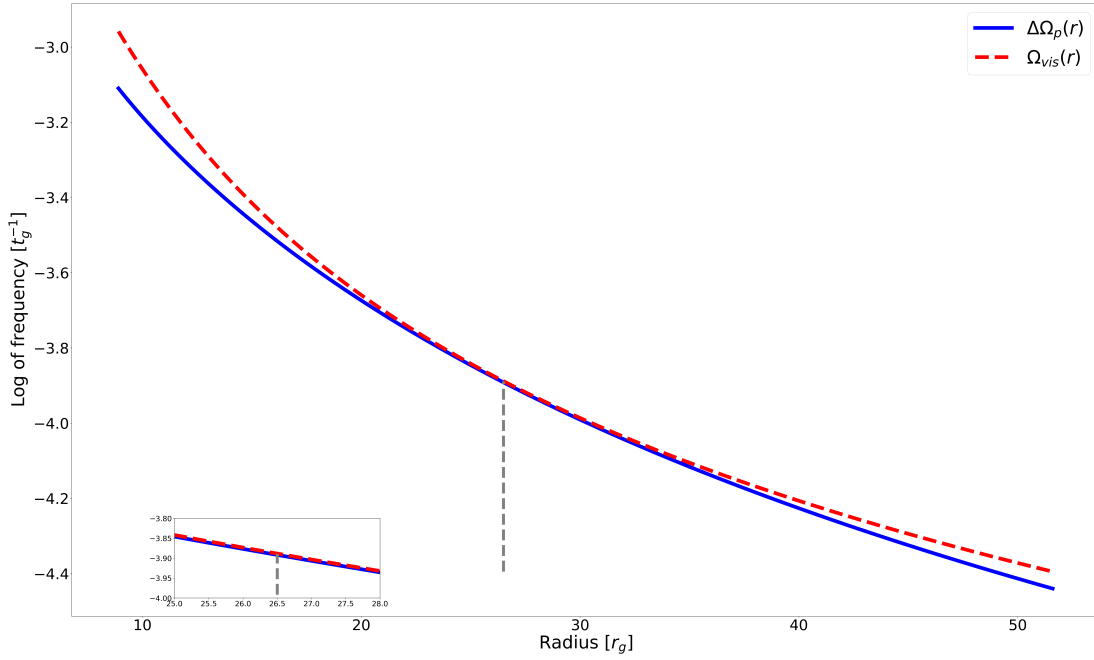


Figure 5: $\Delta\Omega_p(r)$ and $\Omega_{vis}(r)$ for OJ 287. The gray dashed line denotes $r_{sp,0}$.

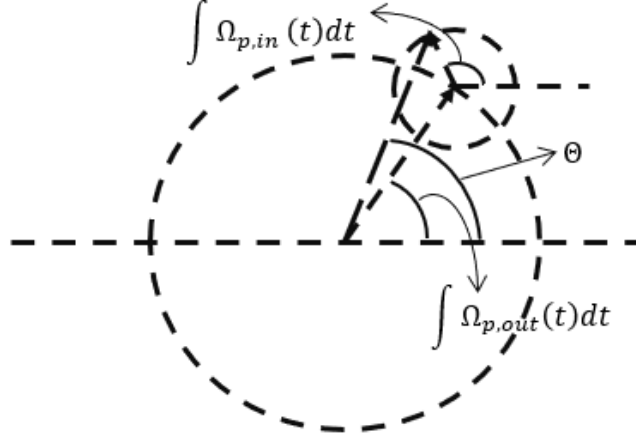


Figure 6: The planform of cork-screw-like precession: the smaller dashed circle depicts the trajectory of jet rotation while the larger one depicts that of precession.

(essentially identical to Eq. (2.13)):

$$\begin{aligned}\Delta\Omega_{p,in}(t,r) &= \Omega_p[r_{in},r] - \Omega_p[r,r_{sp}(t)] , \quad r \in [r_{in},r_{sp}(t)] \\ \Delta\Omega_{p,out}(t,r) &= \Omega_p[r_{sp}(t),r] - \Omega_p[r,r_{out}] , \quad r \in [r_{sp}(t),r_{out}]\end{aligned}\tag{3.1}$$

for the inner disk and the outer disk respectively. Let us analyze the inner disk as an example. We can formally compare $\Delta\Omega_{p,in}(t,r)$ with $\Delta\Omega_p(r)$, whose first terms are the same. Recall that $\Omega_p[r_1,r_2]$ is formally an weighted average of $\omega_p(r)$ which is monotonically decreasing along r . So we always have $\Omega_p[r,r_{sp}(t)] > \Omega_p[r,r_{out}]$. The consequent relation gives $\Delta\Omega_{p,in}(t,r) < \Delta\Omega_p(r) \leq \Omega_{vis}(r)$. It tells that the inner disk cannot overcome the viscosity to further split up into several parts. The situation in the outer disk is the same.

We basically assume that the rotation and precession of jet are synchronous to the precession of inner and outer disk respectively. Under this assumption, the time variation of the precession angle of the jet head should obey (see Fig. 7 for better understanding):

$$\Theta(t) - \Theta_0 = \int_0^t \Omega_{p,out}(t) dt + \psi_{jet} \sin \left[\int_0^t \Omega_{p,in}(t) dt \right]\tag{3.2}$$

where ψ_{jet} is the half opening angle of the jet rotation cone and equals 4° or so for OJ287 [7, 8]. The results for OJ 287 is depicted on Fig. 7 and we compare it with the results of usual cork-screw-like precession (gray dashed line) whose two frequencies are constant. The time varying frequencies make our model distinguishable from the usual cork-screw-like precession and would be verified by more precise observations in the future.

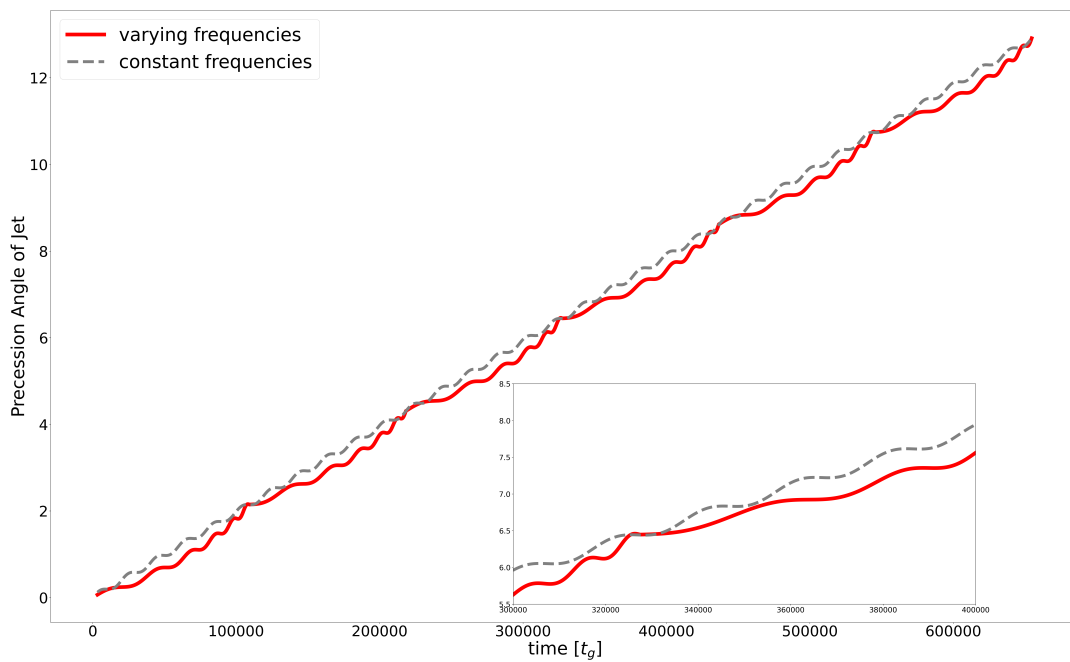


Figure 7: The time variation of precession angle of jet for OJ 287 when considering both precession and rotation. The red line is the result of our model while the gray dashed line is the result that we use $\Omega_{r,obs}$ and $\Omega_{p,obs}$ for the constant frequencies (the usual screw-cork model) directly. We pick $\Theta_0 = 0$ and $\psi_{jet} = 4^\circ$ here.

4 Summary and discussions

In this work, we provided a new analytical model which describes the precession and splitting of a geometrically thin disk. We assumed that the precessions of the split inner and outer disks are in accord with the rotation and precession of relativistic jet respectively. We started from the NT model, which provides the surface mass density, radial velocity distribution, and the viscous timescale. Both the LT effect from the primary BH and the gravitational effect from the secondary BH are considered to induce the disk precession. We proposed the splitting condition of the disk, which requires that the rate of viscous diffusion cannot catch up with the dynamical frequency at a certain layer of fluid. Due to the gravitation, two split disks shrink synchronously and the radial velocity tells the time variation of the split radius, from which we know time variations of the precession frequencies of both the inner and outer disks. We showed that in our model, the split inner and outer disks would not further split up. In order to match the observations, we simply assume that the averaged frequencies of the inner- and outer-disk precessions equal to the observed frequencies (after considering the redshift) of jet rotation and precession respectively. Together with the two equations from the splitting conditions, we have four equations to determine four parameters: the innermost and outermost radii of the disk r_{in} and r_{out} , the initial split radius $r_{\text{sp},0}$ and the inflow speed magnitude β . Based on the observations of OJ 287, we have obtained $(r_{\text{in}}, r_{\text{sp},0}, r_{\text{out}}) \simeq (8.90, 26.5, 51.6)r_g$ and $\beta = 6.33 \times 10^{-3}c$. Additionally, we found that the precession of disk in OJ 287 is dominantly induced by the Lense-Thirring effect from the primary BH.

Moreover, by mapping the averaged frequencies of disks precessions to the frequencies of jet rotation and precession, we plot the time variation of precession angle of jet. The time dependences of frequencies makes our result distinguishable from that of usual cork-screw-like precession and may be detected in the future.

An amount of topics are pending to be investigated in the future and some of them are listed below.

- First and the most importantly, the rationality of the basic assumption we argued that the precessions of disk correspond to the motion of jet is pending to be checked further. According to current GRMHD simulations, the argument is credible that the jet precession is synchronous to the precession of outer disk [25, 26], even in the case that the scale of jet is much larger than that of precessing disk. These simulations assumed that the magnetic field which finally forms the jet comes from the disk only. Although other schemes, such as elliptical accretion disk [41] and single spiral arm in a circular disk [42], may also explain the jet precession, the lack of numerical and observational evidence makes them less trustworthy.

However, no significant evidence showed that the rotation of jet corresponds to the precession of the split inner disk. Numerical results showed that the inner part of jet propagates approximately along the direction of the angular momentum of the inner disk [25], which partly supports our assumption. To be honest, it is an open question where the rotation of jet comes from. There

are other choices not excluded to explain the rotation of jet. For example, it was proposed that the precession of initially tilted magnetic field come from the binary companion instead of disk. However, the most recent simulation shows that the resulting tilted jet should align to the spin axis of BH quickly ($\lesssim 10^3 t_g$) [43]. Besides, the simulations of circum-binary disk and mini-disks, formed when a massive cloud approaches the binary system, provide another possible explanation of the jet rotation [44]. However, these simulations never evolved the accretion systems where the primary BH is much larger than its companion, namely $q \ll 1$, which is the case in OJ 287 [39]. Till now, taking the precession of the split inner disk as the origin of the jet rotation is a relatively better choice.

- Second, as already mentioned in Sect. 2.3, both secular instability [36] and thermal instability [37] suggest that the disk could not keep the structure as the NT model described when radiative pressure is too large. Consequently, the NT model cannot capture the physics in the inner region. That is why we only focused on the medium region in our model. Now a widely accepted model about accretion flow shows that there is a radius of truncation (r_{tr}) outside which the accretion flow forms a geometrically thin disk while inside which it is a geometrically thick and radiative inefficient accretion flow (RIAF) [45]. The value of r_{tr} is around $1 \sim 30 r_{\text{isco}}$, which could probably be determined by observing the X-ray and radio emission near the primary BH [45]. The inner bound of the geometrically thin disk of OJ 287, based on our analysis, should be $8.90 r_g$ within which the accretion flow is highly probable to have a geometrically thick structure. In our model, it is simplified that the mass flowing into the inner boundary ($8.90 r_g$) of the disk is assumed to be absorbed by central BH quickly such that there would be no reaction from this cloud of mass. It is not a completely unreasonable simplification, since in RIAF the plasma is accreted to the event horizon even faster than the gravitational binding energy of the plasma is radiated away. Up to now, it is unclear how the fluid and magnetic field in the region of RIAF contribute to the formation of jet in OJ 287 and backreact the geometrically thin disk outside. It is indispensable to study the dynamics in this region in order to describe the precession of thin disk outside and the corresponding motion of jet in a more accurate way.
- Third, another probable effect that may influence the motion of the disk is the Bardeen-Peterson alignment, which tends to drag the tilted and magnetized disk align to the spin axis of BH [46, 47]. Numerical results of GRMHD also showed that the split inner disk would gradually align to the BH spin when precessing and shrinking [27]. More analyses are necessary to understand this effect better.
- Last but not least, it is also interesting to study the images of a tilted, split accretion disk [48].

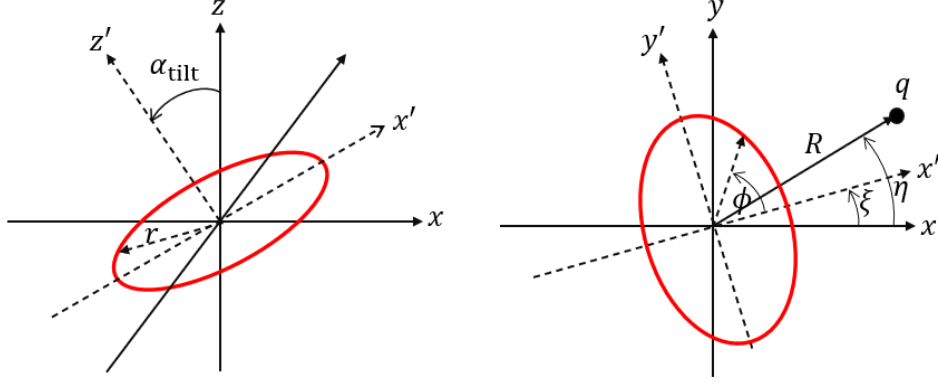


Figure 8: Scheme of gravitational torque on fluid ring, with the primary BH putting on the origin. Axes of BH spin and ring spin are z and z' respectively. ξ denotes the precession angle of ring while η denotes the rotation angle of secondary BH around the origin. x' is the axis crossing the points on the ring with maximal and minimal θ .

Acknowledgement

We are grateful to Yehui Hou, Zhenyu Zhang and Yu Song for useful discussions. The work is partly supported by NSFC Grant No. 12275004.

A Ring precession

Here we show how to get the frequencies in Eq. (2.1) and (2.2) in detail. Consider a steady fluid ring with certain radius spinning around the central BH (see Fig. 8) whose spin axis (z' -axis) has a tiny angle ($\alpha_{\text{tilt}} \ll 1$) with the BH spin (z -axis). Fluid elements on the ring are all assumed to rotate around z' -axis with a frequency Ω_ϕ close to the Keplerian frequency. We set $\dot{r} = 0$, $\dot{\theta} \ll \dot{\phi}$ and $d\phi/dt \equiv \Omega_\phi \simeq (r^{3/2} + a)^{-1}$ (co-rotating case only). Now let us study how the primary BH on the center and the secondary BH in a long distance induce the precession of fluid ring separately.

A.1 Lense-Thirring Effect

Consider the motion of fluid element along θ . We purely consider the effect from primary BH, so that the equation of motion (EoM) in θ direction should just be the geodesic equation:

$$\frac{d}{d\tau} \left(\frac{d\mathcal{L}}{d\dot{\theta}} \right) = \frac{d\mathcal{L}}{d\theta} \quad (\text{A.1})$$

Here \mathcal{L} is the Lagrangian of a probe particle moving in the Kerr spacetime and the dot means $\frac{d}{d\tau}$. The detailed expression of Eq. (A.1) is

$$\begin{aligned} \text{LHS} &= \frac{d}{d\tau}(\Sigma\dot{\theta}), \\ \text{RHS} &\approx \frac{2\sin\theta\cos\theta}{\Sigma^2} \left\{ a^2 r \dot{t}^2 - 2ar(r^2 + a^2)\dot{t}\dot{\phi} + \left[\frac{(r^2 + a^2)\Sigma^2}{2} + a^2 r \sin^2\theta(\Sigma + r^2 + a^2) \right] \dot{\phi}^2 \right\} \end{aligned} \quad (\text{A.2})$$

where $\Sigma = r^2 + a^2 \cos^2\theta$. In the second equation of Eq (A.2) we discard all terms of $\mathcal{O}(\dot{r}, \dot{\theta})$. As t is independent of τ , we can divide \dot{t} on both sides and exchange $d/d\tau$ to d/dt . Furthermore, as $\sin\theta \simeq 1$, $\cos\theta \simeq \pi/2 - \theta \equiv \alpha$ and also $r \gg a^2 \cos^2\theta$, the EoM of θ can be simplified as:

$$\frac{d^2\alpha}{dt^2} \approx -\frac{\Omega_\phi^2}{r^6} \left[\frac{2a^2 r}{\Omega_\phi^2} - \frac{4ar(r^2 + a^2)}{\Omega_\phi} + (r^6 + a^2 r^4 + 2a^2 r^3 + 2a^3 r) \right] \alpha. \quad (\text{A.3})$$

The equation above is a specific form of: $\frac{d^2\alpha}{dt^2} = -\omega_\theta^2 \alpha$. It describes a sinusoidal vibration along α (or θ equivalently) as long as $\omega_\theta^2 > 0$. It is easy to check that $\omega_\theta = \Omega_\phi$ when $a = 0$, which tells that the fluid elements rotate around a Schwarzschild BH stably (without any precession or nutation).

Generally, there are three kinds of motion that Eq. (A.3) can describe. First, if $\omega_\theta^2 > 0$ and $\omega_\theta < \Omega_\phi$, it describes that a fluid element moves along a ring which is precessing in the direction of z with a frequency of $\Omega_\phi - \omega_\theta$. Second, if $\omega_\theta^2 > 0$ while $\omega_\theta > \Omega_\phi$, the fluid element traces a ring that is precessing in the direction of $-z$ with a frequency of $\omega_\theta - \Omega_\phi$. Third, when $\omega_\theta^2 < 0$, Eq. (A.3) is never an EoM of a sinusoidal motion. A stable solution in this case shows the angular momentum of the fluid element align to the BH spin.

When we substitute $\Omega_\phi \simeq \Omega_K = (r^{3/2} + a)^{-1}$ into Eq. (A.3), we get:

$$\omega_\theta^2 = \Omega_K^2 \left(1 - 4ar^{-\frac{3}{2}} + 3a^2 r^{-2} \right). \quad (\text{A.4})$$

It is easy to check that, in this case, $0 < \omega_\theta^2 < \Omega_\phi^2$ in the region outside the event horizon, so the fluid elements moves along a ring which is precessing in the direction of z with a frequency shown in Eq. (2.1).

If the ring is in retrograde motion with respect to the spinning of the black hole, there is

$$\omega_\theta^2 = \Omega_K^2 \left(1 + 4ar^{-\frac{3}{2}} + 3a^2 r^{-2} \right)$$

where $\Omega_K = -(r^{3/2} - a)^{-1}$. In this case, the ring undergoes a precession in the direction of z as well.

A.2 Secondary BH

Now let us consider the gravitational effect on the ring from a secondary BH with a mass ratio q to the primary BH mass, locating on the equatorial plane in a distance of R away from the center. We analyze this problem in Cartesian coordinates with $x - y$ plane on the equatorial (see the right panel in

Fig. 8). The polar angle (angle of projected position vector with x -axis on $x-y$ plane) of secondary BH is η while the polar angle of the node of tilted ring (point with minimal θ on the ring) is ξ . The relativistic effect can be neglected since the secondary BH is much tinier ($q \ll 1$ namely) than the primary one. We approximately set

$$1 \ll r \ll R \quad , \quad \dot{\xi} \ll \dot{\eta} \ll \dot{\phi} \simeq \Omega_K. \quad (\text{A.5})$$

The dots on the top means $\frac{d}{dt}$ for now. In other words, we consider the ring which is not too close to the primary BH so that the Lense-Thirring effect is not strong. It is unnecessary to consider the effect of secondary BH acting on the ring with a small radius because the Lense-Thirring effect from the primary BH is dominant. Moreover, we approximately set the separation of two BHs is much larger than the radius of the ring for calculation simplicity, which is the case for some accretion systems with secondary BHs, say, $R \simeq 10^3 r_g$ in OJ 287 [39] and $R \simeq 10^4 r_g$ in M81 [11].

The torque acting on fluid elements of the ring is simply

$$\vec{\tau} = \vec{r} \times \vec{F} = q\vec{r} \times \frac{\vec{R} - \vec{r}}{|\vec{R} - \vec{r}|^3} \quad (\text{A.6})$$

with

$$\vec{R} = R(\cos \eta, \sin \eta, 0) \quad , \quad \vec{r} = r(\cos \alpha_{\text{tilt}} \cos(\phi + \xi), \sin(\phi + \xi), \sin \alpha_{\text{tilt}} \cos(\phi + \xi)). \quad (\text{A.7})$$

We can expand Eq. (A.6) by powers of r/R and then do integration over ϕ . Keeping the leading-order non-trivial terms only, we get

$$\begin{aligned} \tau_x &= -\frac{3\pi q}{4} \frac{r^2}{R^3} [\sin 2(\eta - \xi) \cos \xi + 2 \cos^2(\eta - \xi) \sin \xi] \sin 2\alpha_{\text{tilt}}, \\ \tau_y &= -\frac{3\pi q}{4} \frac{r^2}{R^3} [\sin 2(\eta - \xi) \sin \xi - 2 \cos^2(\eta - \xi) \cos \xi] \sin 2\alpha_{\text{tilt}}, \\ \tau_z &= \frac{3\pi q}{2} \frac{r^2}{R^3} \sin 2(\eta - \xi) [\cos^2 \alpha_{\text{tilt}} - 1]. \end{aligned} \quad (\text{A.8})$$

It is obvious that the torque acting on the ring depends on the position of secondary BH. As we have already set that the (potential) precession of the ring is much slower than the orbiting of secondary BH, we could just consider the averaged effect:

$$\begin{aligned} \langle \tau_x \rangle_\eta &= -\frac{3\pi q}{4} \frac{r^2}{R^3} \sin \xi \sin 2\alpha_{\text{tilt}}, \\ \langle \tau_y \rangle_\eta &= -\frac{3\pi q}{4} \frac{r^2}{R^3} \cos \xi \sin 2\alpha_{\text{tilt}}, \\ \langle \tau_z \rangle_\eta &= 0. \end{aligned} \quad (\text{A.9})$$

It is easy to get the total angular momentum of the fluid ring:

$$\vec{L} = 2\pi r^2 \Omega_\phi (-\cos \xi \sin \alpha_{\text{tilt}}, -\sin \xi \sin \alpha_{\text{tilt}}, \cos \alpha_{\text{tilt}}). \quad (\text{A.10})$$

Then by equaling $\langle \tau_x \rangle_\eta$ to \dot{L}_x (or $\langle \tau_y \rangle_\eta$ to \dot{L}_y identically), we get the precession frequency shown in Eq. (2.2). Different from the Lense Thirring effect, the effect of secondary BH inducing a precession is a holistic effect on the fluid ring. No precession would happen if we purely consider one fluid element. The precession happens because of the difference between gravitational forces acting on different parts of the ring. This requires that the gravitation of the secondary BH never deforms the ring.

References

- [1] P. Padovani et al., “Active galactic nuclei: what’s in a name?,” *Astron. Astrophys. Rev.* **25** no. 1, (2017) 2, [arXiv:1707.07134](https://arxiv.org/abs/1707.07134) [astro-ph.GA].
- [2] A. Caproni and Z. Abraham, “Jet precession and its observational evidence: The cases of 3c 345 and 3c 120,” *Proceedings of the International Astronomical Union* **2004** no. IAUS222, (2004) 83–84.
- [3] A. Caproni and Z. Abraham, “Precession in the inner jet of 3c 345,” *The Astrophysical Journal* **602** no. 2, (Feb, 2004) 625. <https://dx.doi.org/10.1086/381195>.
- [4] A. Caproni and Z. Abraham, “Can long - term periodic variability and jet helicity in 3C 120 be explained by jet precession?,” *Mon. Not. Roy. Astron. Soc.* **349** (2004) 1218, [arXiv:astro-ph/0312407](https://arxiv.org/abs/astro-ph/0312407).
- [5] A. Caproni, H. J. Mosquera Cuesta, and Z. Abraham, “Observational evidence of spin-induced precession in active galactic nuclei,” *Astrophys. J. Lett.* **616** (2004) L99–L102, [arXiv:astro-ph/0410450](https://arxiv.org/abs/astro-ph/0410450).
- [6] S.-M. Liu and F. Melia, “Spin - induced disk precession in the supermassive black hole at the Galactic Center,” *Astrophys. J. Lett.* **573** (2002) L23, [arXiv:astro-ph/0205487](https://arxiv.org/abs/astro-ph/0205487).
- [7] S. Britzen, C. Fendt, G. Witzel, S.-J. Qian, I. N. Pashchenko, O. Kurtanidze, M. Zajaček, G. Martinez, V. Karas, M. Aller, H. Aller, A. Eckart, K. Nilsson, P. Arévalo, J. Cuadra, M. Subroweit, and A. Witzel, “OJ287: deciphering the ‘Rosetta stone of blazars’,” *Monthly Notices of the Royal Astronomical Society* **478** no. 3, (04, 2018) 3199–3219, <https://academic.oup.com/mnras/article-pdf/478/3/3199/25062878/sty1026.pdf>. <https://doi.org/10.1093/mnras/sty1026>.
- [8] S. Britzen, M. Zajaček, Gopal-Krishna, C. Fendt, E. Kun, F. Jaron, A. Sillanpää, and A. Eckart, “Precession-induced variability in agn jets and oj 287,” *The Astrophysical Journal* **951** no. 2, (Jul, 2023) 106. <https://dx.doi.org/10.3847/1538-4357/acbbbc>.
- [9] von Fellenberg, S. D., Janssen, M., Davelaar, J., Zajaček, M., Britzen, S., Falcke, H., Körding, E., and Ros, E., “Radio jet precession in m 81*,” *Astron. Astrophys.* **672** (2023) L5. <https://doi.org/10.1051/0004-6361/202245506>.
- [10] W. Jiang, Z. Shen, D. Jiang, I. Martí-Vidal, and N. Kawaguchi, “Vlbi imaging of m81* at $\lambda = 3.4$ mm with source-frequency phase-referencing,” *The Astrophysical Journal Letters* **853** no. 1, (Jan, 2018) L14. <https://dx.doi.org/10.3847/2041-8213/aaa755>.

- [11] W. Jiang, Z. Shen, I. Martí-Vidal, Z. Yan, L. Huang, R. Gold, Y.-P. Li, F. Xie, and N. Kawaguchi, “Observational Evidence of a Centi-parsec Supermassive Black Hole Binary Existing in the Nearby Galaxy M81,” [arXiv:2312.01328 \[astro-ph.GA\]](#).
- [12] Y. Cui et al., “Precessing jet nozzle connecting to a spinning black hole in M87,” [Nature](#) **621** (2023) 711–715, [arXiv:2310.09015 \[astro-ph.HE\]](#).
- [13] M. Kam, J. A. Hodgson, J. Park, M. Kino, H. Nagai, S. Trippe, and A. Y. Wagner, “Evolution of the Termination Region of the Parsec-Scale Jet of 3C 84 Over the Past 20 Years,” [arXiv:2312.13666 \[astro-ph.HE\]](#).
- [14] R. D. Blandford and R. L. Znajek, “Electromagnetic extraction of energy from Kerr black holes.,” [Mon. Not. Roy. Astron. Soc.](#) **179** (May, 1977) 433–456.
- [15] R. D. Blandford and D. G. Payne, “Hydromagnetic flows from accretion disks and the production of radio jets.,” [Mon. Not. Roy. Astron. Soc.](#) **199** (June, 1982) 883–903.
- [16] S. W. Davis and A. Tchekhovskoy, “Magnetohydrodynamics Simulations of Active Galactic Nucleus Disks and Jets,” [Ann. Rev. Astron. Astrophys.](#) **58** (2020) 407–439, [arXiv:2101.08839 \[astro-ph.HE\]](#).
- [17] S. Kato, “Trapped One-Armed Corrugation Waves and QPO’s,” [Publications of the Astronomical Society of Japan](#) **42** (Feb., 1990) 99–113.
- [18] J. I. Katz, S. F. Anderson, B. Margon, and S. A. Grandi, “Nodding motions of accretion rings and disks : a short-term period in SS 433.,” [Astrophysical Journal](#) **260** (Sept., 1982) 780–793.
- [19] P. C. Fragile and P. Anninos, “Hydrodynamic Simulations of Tilted Thick-Disk Accretion onto a Kerr Black Hole,” [The Astrophysical Journal](#) **623** no. 1, (Apr., 2005) 347–361, [arXiv:astro-ph/0403356 \[astro-ph\]](#).
- [20] P. C. Fragile, O. M. Blaes, P. Anninos, and J. D. Salmonson, “Global General Relativistic Magnetohydrodynamic Simulation of a Tilted Black Hole Accretion Disk,” [The Astrophysical Journal](#) **668** no. 1, (Oct., 2007) 417–429, [arXiv:0706.4303 \[astro-ph\]](#).
- [21] A. D. Bollimpalli, P. C. Fragile, W. J. Dewberry, and W. Kluźniak, “Truncated, Tilted Discs as a Possible Source of Quasi-Periodic Oscillations,” [arXiv:2312.14876 \[astro-ph.HE\]](#).
- [22] S. M. Ressler, C. J. White, and E. Quataert, “Wind-fed GRMHD simulations of Sagittarius A*: tilt and alignment of jets and accretion discs, electron thermodynamics, and multiscale modelling of the rotation measure,” [Mon. Not. Roy. Astron. Soc.](#) **521** no. 3, (2023) 4277–4298, [arXiv:2303.15503 \[astro-ph.HE\]](#).

- [23] J. C. McKinney, A. Tchekhovskoy, and R. D. Blandford, “Alignment of Magnetized Accretion Disks and Relativistic Jets with Spinning Black Holes,” *Science* **339** (2013) 49–52, [arXiv:1211.3651 \[astro-ph.CO\]](#).
- [24] M. T. P. Liska, K. Chatterjee, D. Issa, D. Yoon, N. Kaaz, A. Tchekhovskoy, D. van Eijnatten, G. Musoke, C. Hesp, V. Rohoza, S. Markoff, A. Ingram, and M. van der Klis, “H-AMR: A New GPU-accelerated GRMHD Code for Exascale Computing with 3D Adaptive Mesh Refinement and Local Adaptive Time Stepping,” *The Astrophysical Journal Supplement Series* **263** no. 2, (Dec., 2022) 26, [arXiv:1912.10192 \[astro-ph.HE\]](#).
- [25] M. Liska, C. Hesp, A. Tchekhovskoy, A. Ingram, M. van der Klis, and S. Markoff, “Formation of Precessing Jets by Tilted Black-hole Discs in 3D General Relativistic MHD Simulations,” *Mon. Not. Roy. Astron. Soc.* **474** no. 1, (2018) L81–L85, [arXiv:1707.06619 \[astro-ph.HE\]](#).
- [26] M. Liska, C. Hesp, A. Tchekhovskoy, A. Ingram, M. van der Klis, and S. B. Markoff, “A phase lag between disc and corona in GRMHD simulations of precessing tilted accretion discs,” *New Astronomy* **101** (July, 2023) 102012, [arXiv:1901.05970 \[astro-ph.HE\]](#).
- [27] M. Liska, C. Hesp, A. Tchekhovskoy, A. Ingram, M. van der Klis, S. B. Markoff, and M. Van Moer, “Disc tearing and Bardeen–Petterson alignment in GRMHD simulations of highly tilted thin accretion discs,” *Mon. Not. Roy. Astron. Soc.* **507** no. 1, (2021) 983–990, [arXiv:1904.08428 \[astro-ph.HE\]](#).
- [28] N. I. Shakura and R. A. Sunyaev, “Black holes in binary systems. Observational appearance,” *Astron. Astrophys.* **24** (1973) 337–355.
- [29] Black-hole accretion disks. Jan., 1998.
- [30] B. Mishra, M. C. Begelman, P. J. Armitage, and J. B. Simon, “Strongly magnetized accretion discs: structure and accretion from global magnetohydrodynamic simulations,” *Mon. Not. Roy. Astron. Soc.* **492** no. 2, (2020) 1855–1868, [arXiv:1907.08995 \[astro-ph.HE\]](#).
- [31] I. D. Novikov and K. S. Thorne, “Astrophysics of black holes.,” in Black Holes (Les Astres Occlus), pp. 343–450. Jan., 1973.
- [32] D. N. Page and K. S. Thorne, “Disk-Accretion onto a Black Hole. Time-Averaged Structure of Accretion Disk,” *Astrophysical Journal* **191** (July, 1974) 499–506.
- [33] J. Lense and H. Thirring, “Über den Einfluß der Eigenrotation der Zentralkörper auf die Bewegung der Planeten und Monde nach der Einsteinschen Gravitationstheorie,” *Physikalische Zeitschrift* **19** (Jan., 1918) 156.

- [34] C. E. J. M. L. J. Terquem, “The response of accretion disks to bending waves: Angular momentum transport and resonances,” *The Astrophysical Journal* **509** no. 2, (Dec, 1998) 819. <https://dx.doi.org/10.1086/306505>.
- [35] M. R. Bate, I. A. Bonnell, C. J. Clarke, S. H. Lubow, G. I. Ogilvie, J. E. Pringle, and C. A. Tout, “Observational implications of precessing protostellar discs and jets,” *Mon. Not. Roy. Astron. Soc.* **317** (2000) 773, [arXiv:astro-ph/0005333](https://arxiv.org/abs/astro-ph/0005333).
- [36] A. P. Lightman and D. M. Eardley, “Black Holes in Binary Systems: Instability of Disk Accretion,” *Astrophys. J. Lett.* **187** (1974) L1.
- [37] J. E. Pringle, “Thermal Instabilities in Accretion Discs,” *Mon. Not. Roy. Astron. Soc.* **177** no. 1, (10, 1976) 65–71, <https://academic.oup.com/mnras/article-pdf/177/1/65/9333393/mnras177-0065.pdf>. <https://doi.org/10.1093/mnras/177.1.65>.
- [38] F.-K. Liu and X.-B. Wu, “Black hole mass and binary model for BL Lac object OJ 287,” *Astron. Astrophys.* **388** (2002) L48, [arXiv:astro-ph/0212475](https://arxiv.org/abs/astro-ph/0212475).
- [39] M. J. Valtonen *et al.*, “Observational Implications of OJ 287’s Predicted 2022 Disk Impact in the Black Hole Binary Model,” *Galaxies* **11** no. 4, (2023) 82, [arXiv:2308.01878](https://arxiv.org/abs/2308.01878) [[astro-ph.HE](https://arxiv.org/abs/astro-ph.HE)].
- [40] M. J. Valtonen *et al.*, “Primary black hole spin in OJ287 as determined by the General Relativity centenary flare,” *Astrophys. J. Lett.* **819** no. 2, (2016) L37, [arXiv:1603.04171](https://arxiv.org/abs/1603.04171) [[astro-ph.HE](https://arxiv.org/abs/astro-ph.HE)].
- [41] M. Eracleous, M. Livio, J. P. Halpern, and T. Storchi-Bergmann, “Elliptical Accretion Disks in Active Galactic Nuclei,” *The Astrophysical Journal* **438** (Jan., 1995) 610.
- [42] T. Storchi-Bergmann, R. Nemmen da Silva, M. Eracleous, J. P. Halpern, A. S. Wilson, A. V. Filippenko, M. T. Ruiz, R. C. Smith, and N. M. Nagar, “Evolution of the Nuclear Accretion Disk Emission in NGC 1097: Getting Closer to the Black Hole,” *The Astrophysical Journal* **598** no. 2, (Dec., 2003) 956–968, [arXiv:astro-ph/0308327](https://arxiv.org/abs/astro-ph/0308327) [[astro-ph](https://arxiv.org/abs/astro-ph)].
- [43] S. Selvi, O. Porth, B. Ripperda, and L. Sironi, “Current sheet alignment in oblique black hole magnetospheres – a black hole pulsar?,” [arXiv:2402.16055](https://arxiv.org/abs/2402.16055) [[astro-ph.HE](https://arxiv.org/abs/astro-ph.HE)].
- [44] F. G. Goicovic, J. Cuadra, A. Sesana, F. Stasyszyn, P. Amaro-Seoane, and T. L. Tanaka, “Infalling clouds on to supermassive black hole binaries – I. Formation of discs, accretion and gas dynamics,” *Mon. Not. Roy. Astron. Soc.* **455** no. 2, (2016) 1989–2003, [arXiv:1507.05596](https://arxiv.org/abs/1507.05596) [[astro-ph.HE](https://arxiv.org/abs/astro-ph.HE)].
- [45] B. You, X. Cao, Z. Yan, J.-M. Hameury, B. Czerny, Y. Wu, T. Xia, M. Sikora, S.-N. Zhang, P. Du, and P. T. Zycki, “Observations of a black hole x-ray binary indicate formation of a magnetically arrested disk,” *Science* **381** no. 6661, (2023) 961–964,

<https://www.science.org/doi/pdf/10.1126/science.abo4504>.

<https://www.science.org/doi/abs/10.1126/science.abo4504>.

- [46] J. M. Bardeen and J. A. Petterson, “The Lense-Thirring Effect and Accretion Disks around Kerr Black Holes,” [*Astrophys. J. Lett.* **195** \(1975\) L65](#).
- [47] A. R. King and J. P. Lasota, “Magnetic alignment of rotating black holes and accretion discs,” [*Astronomy and Astrophysics* **58** no. 1-2, \(June, 1977\) 175–179](#).
- [48] K. Chatterjee, Z. Younsi, M. Liska, A. Tchekhovskoy, S. B. Markoff, D. Yoon, D. van Eijnatten, C. Hesp, A. Ingram, and M. van der Klis, “Observational signatures of disc and jet misalignment in images of accreting black holes,” [*Mon. Not. Roy. Astron. Soc.* **499** no. 1, \(2020\) 362–378](#), [arXiv:2002.08386 \[astro-ph.GA\]](#).